Physics of Failure

K. V. Jata and T.A. Parthasarathy*
Air Force Research Laboratory,
Materials and Manufacturing Directorate, AFRL/MLL
Wright-Patterson AFB, OH 45433-7817
* UES, Inc., Dayton OH 45432

ABSTRACT

The aerospace industry is developing structural health monitoring systems to reliably detect, locate and quantify damage in components and use the identified damage feature to make a decision on whether to repair or replace the component or for prognosis of the remaining useful component life and system performance. Mission-readiness, minimization of costs due to unnecessary tear downs and NDE (Nondestructive Evaluation) inspections as well as safety are some of the major goals of systems health monitoring. Current structural health monitoring systems focus on detecting the damage at component level and focus less on the failure of the material. It is anticipated that microstructure-based methods will offer higher quality prognosis and avoid unexpected and expensive failures. Knowledge of the physical mechanisms through which materials fail might motivate the NDE and SHM (Structural Health Monitoring) engineers to enter the next phase of health monitoring. Methods based on vibration signature of the structure, for example are useful in detecting damage at a global level and help predict damage level in a component; however such methods do not furnish information of failure processes at a microstructure level. The purpose of this paper is to help move the NDE and the SHM community in the direction of adopting failure mechanisms at a microstructure level whether it be in the area of damage diagnostics or prognosis. Hopefully, the discussion of various prominent failure mechanisms in structural materials presented in this paper will serve that purpose and in the future this paper will serve as a reference for either developing sensors based on material failure at a microstructure scale or for performing prognosis using microstructural parameters. Understanding of material degradation and failure mechanisms at a microstructure scale for a given set of operational conditions can be broadly termed as "Physics of Failure." On the diagnostics side, it will be helpful to design new sensors based on an interpretation of a failure mode rather than simply suggesting that some sort of failure has occurred. For prognosis of remaining useful life it will be beneficial to not only quantify the damage but also to know the physics of damage initiation and progression to perform microstructure-based life prediction modeling. Similarly, knowing the physics of failure at spatial and temporal levels for a structure would be beneficial for structural repair and (or) better material substitution. The failure process in materials is a vast and complex field and to summarize it is a challenging task. The reader must note that this paper is an attempt to present a comprehensive view of the "Physics of Failure," at the possible risk of oversimplification. This is thus a first-level guide to the failure mechanisms that dominate failure of components using state-of-the-art materials.

INTRODUCTION

Currently very little research is being performed in the area of development of new sensors that can detect damage at a microstructure scale. Micro crack nucleation, macro crack formation and crack extension are well understood in metals, ceramics, ceramic matrix composites (CMC), polymer matrix composites and carbon-carbon (C-C) composites. Most of this understanding is based on tests on laboratory samples in well controlled environments and many new materials have been developed in recent years based on such understanding. However, when alloys are scaled up from laboratory samples to large-scale product forms or when the environment is changed from that of a laboratory to that of a near-operational environment, failure

modes can change significantly. These deviations arise because chemical composition is not as easy to control in large ingots (e.g. 10,000 lb.) as in a small laboratory size ingot (e.g. 100 lb.) Similarly, larger variations in properties occur while processing large ingots during component manufacturing (e.g. mid thickness properties can vary substantially from surface properties). Fracture modes can thus be different in components as compared to that in the laboratory samples. Life prediction models also exist for many of the materials to predict their fatigue life in laboratory setting and to some extent in operational/service environments. Here again chemical composition variations, impurity segregation, and manufacturing processes can result in microstructures different from that in the lab samples. This combined with unanticipated changes or ill-defined operational environments can lead to new fracture modes and inaccurate estimations of service life. A large uncertainty can, therefore be introduced through variations in microstructure and operational environment. There is a lack of connection between different levels of failures-from the microstructure level to the meso scale to the macro scale levels. Mathematical frameworks and software algorithms are practically absent to connect these various length scales, making the predictions very difficult. So, most of the life prediction approaches are overly conservative and structures that are employed have large safety margins resulting in less weight benefits than desired. To reduce the design margin and to predict life more accurately, in recent years there has been an increasing emphasis on prognosis of remaining useful life of components on physics-based damage models or models based on microstructure and constitutive properties. Such approaches are clearly needed to predict not only incipient damage nucleation and propagation, but also how damage initiated in the first place. Understanding how the damage has nucleated and how the damage will propagate, under loads and service environment requires some knowledge of materials behavior and the effect of microstructure constituents on properties of interest. In the case of prognosis, efforts are underway to develop life prediction models that incorporate microstructure, physics–based damage models and crystal plasticity models.

While many materials models have been developed over the past several decades, without proper detection methods, these models will remain under-used by designers. For example, processing of materials has advanced to such a level, that the detection of pre-existing flaws in these materials is a real challenge. However materials science has evolved over the years to be able to link microstructural features to the initiation and growth of damage. Thus, measurement of microstructural features and their evolution during service represents a significant opportunity for the next generation of NDE techniques. It is hoped that knowledge of the physics of failure in materials will motivate NDE engineers to devise these next generation methodologies and instrumentation. The physics of failure deals with failure of materials at a microstructure level that are very small scale events; however, over time these micro-scale events ultimately hinder a component from performing its function through failure. Knowledge of failure mechanisms has been successfully exploited in developing new materials with improved properties by essentially eliminating or modifying the microstructural constituents responsible for initiating failures in a material. To assess damage and predict remaining useful life of a component and to use the entire capability of a given material, it is critical to convey the physics of failure of the material along with the material constitutive properties to the designers involved in selecting materials and sizing components. Similarly, to build better diagnostic systems capable of diagnosing damage at a microstructure level, physics of failure needs to be understood because damage nucleates at microstructure inhomogeneities. The smaller the scale of the inhomogeneity, the smaller the scale of the initial damage features. This paper will attempt to summarize failure modes in metals and Ceramic Matrix Composites (CMC's) that can be used as a first step in developing new sensors to detect damage and aid prognosis methods for life prediction.

PHYSICS OF FAILURE OF METALS

1. HIGH LEVEL CLASSIFICATION

At a high level, failure in metals or alloys can be broadly classified as shown in Table 1 under three categories, (I) deformation, (ii) fracture and (iii) material loss.

1.1 DEFORMATION

A metallic alloy can fail to perform an assigned function due to excessive deformation either arising from inferior yield strength at ambient temperatures or through excessive creep at high temperatures. For instance, improper selection of material higher operational temperatures which exceeds the capability of the material strength may lead to failure through deformation. As shown in Table 1, deformation failures depend on either yield or creep phenomenon and are fundamentally related to stress. Most of the plasticity associated with yield is athermal, whereas in the case of creep thermal plasticity plays a key role. Creep deformation resulting from the applied stress at temperature is a function of the time. Many of the components that undergo creep deformation are therefore designed not to exceed a certain amount of deformation under a given applied load over a specified time interval.

1.2 FRACTURE

Fracture is a very broad term; however at a high level it can be classified as static, dynamic and creep rupture. Static fracture occurs in fracture mechanics specimens or in uniaxially stressed tensile coupons due to overloads or over-stressing the material. Stress is the fundamental parameter that governs static fracture; cyclic loads are absent in static fracture situations. Total elongation to failure in a test coupon is a first tier property often measured on inexpensive tensile coupons, but fracture toughness, K_{1c} or J_{1c}, is a much more suitable parameter when designing fracture-critical components as the fracture toughness provides the critical crack size that the structure can sustain for a given applied stress. In the case of fracture mechanics specimens, stress is also a fundamental parameter and one can adjust the applied stress so that the critical crack size is not reached during service to prevent a failure.

Creep rupture is the second major mode of failure that can occur in high temperature rotating or static components. Rotating engine parts such as turbine blades are under the influence of centrifugal force at high temperatures for prolonged periods of time. Excessive creep deformation may initially occur but continued exposure may lead to creep-rupture, which may be due to either a poor selection of material or a poor definition of operational environment. Creep rupture is a design parameter commonly employed in the design of pipes carrying liquid through a boiler or a nuclear reactor. Stress in the pipe not only reduces the cross section of the pipe but also promotes formation of small cavities over a period of time at the operating temperature. The cavities form either intra-granularly or at the grain boundaries, which eventually link up resulting in failure through creep rupture. The formation of cavities is a thermally activated process.

1.3 DYNAMIC FATIGUE

Major attention has been paid over the last few decades to the field of fatigue as the majority of failures (even today) occur under fatigue loading. When a component is subjected to repeat stress-cycles, fatigue failure occurs with cyclic plasticity accumulation. Fatigue can be simulated either by using smooth bars that can be subjected either to stress-controlled fatigue or strain-controlled fatigue. Smooth bars represent failure in the absence of cracks in the structure. In the stress-controlled fatigue situation (high cycle fatigue), applied stress is below the yield stress and very little plasticity is accumulated. In the case of strain-controlled fatigue (also known as low cycle fatigue), applied stresses are beyond the yield stress of the material and the accumulated plasticity is considerably higher than that in the high cycle fatigue, resulting in fewer cycles to failure. Fracture mechanics tests are conducted for the evaluation of fatigue crack resistance in the presence of a sharp crack. Current fracture mechanics approaches represent

atomically sharp cracks or microstructural inhomogenities as stress concentrators and crack nucleation sites. In all fatigue situations, the number of cycles and applied stress range (maximum stress minus minimum stress) play a key role. In the case of the fracture mechanics approach, the stress intensity range is the parameter that extends the crack and fatigue crack growth rates which dictate the remaining life. The number of cycles to failure are computed for a given crack size to reach a critical size. Presence of small cracks (equivalent to the size of a microstructure unit such as grain size) is detrimental to engine components and therefore much attention has been paid in the literature to studying small crack behavior in engine component materials. Here stress and the number of fatigue cycles are first order parameters to be considered.

Table. 1 Classification of failure modes in metallic alloys

Deformation	Yield	athermal plasticity	f (stress)
	Creep	thermally activated plasticity	f (temp, time, stress)
Fracture	Static	athermal / acyclic fracture	f (stress)
	Creep rupture	thermally activated cavitation leading to fracture	f (temp, time, stress)
	Dynamic fatigue	Cyclic plasticity leading to nucleation/growth of cracks	f (cyclic stress, cycle#)
Material Loss	Corrosion	athermal loss of material	f (time, environment)
	Oxidation	thermally activated	f (time, temp, O_2 pres)

1.4 MATERIAL LOSS

The last failure mode listed in Table 1 is the material loss of a metal that can occur either due to corrosion or due to high temperature oxidation. (In this paper the discussion is mostly on corrosion in aqueous environments. Material loss can occur through erosion, fretting and wear but these mechanisms will not be discussed here). Loss of material in a corrosive environment as shown in Table 1, is referred to as general or uniform corrosion and is strongly dependent on the environment and time of exposure. Many times components undergoing such corrosion are either repaired by grinding out the corrosion, or replaced after a certain amount of material loss occurs beyond the amount allowed in the material for structural specifications of the component. Time of exposure to the corrosive environment is a key parameter. Many other corrosion mechanisms exist that will be discussed in the next level of failure process. Material loss at high temperatures usually involves material oxidation. For a first order approximation, material loss by such a mechanism will depend on the partial pressure of O_2 and time and temperature of exposure. Material loss could be rapid in this situation compared to the corrosion process.

2. SECOND LEVEL CLASSIFICATION

In this section the factors associated with the first-level fracture mechanisms: yield, creep, static fracture, creep rupture, dynamic fatigue, corrosion and oxidation---are discussed. The goal here is to provide a discussion of the microstructure parameters that control these material failure modes. As will be noted below, most of the fundamental microstructure parameters such as grain size, strengthening precipitates and second phase particle content are the dominant parameters.

2.1 DEFORMATION DUE TO YIELD

Depending on the service temperature, the two deformation characteristics of a material that can lead to failure are the yield strength and creep resistance. As mentioned above, failure in this particular case can mean excessive deformation in the material that leads to inoperability of the component due to excessive elongation.

If one needs to monitor failures due to excessive yielding then one must monitor the athermal plasticity of the material in question. From a microstructure point of view, the logical question then is "what material factors control the athermal plasticity," or "what material factors does one need to sense or monitor regarding athermal plasticity." For traditional structural engineering materials, the yield strength is inversely proportional to the square root of the grain size (a fundamental microstructure parameter) through the Hall-Petch relation:

$$\sigma_y = \sigma_0 + kd^{-n} \qquad \ldots \qquad (1)$$

where σ_y is the yield strength, σ_0 is the yield strength of a single crystal, d the grain size, k the Hall-Petch coefficient, and n is the Hall-Petch slope, is typically equal to 0.5.

In conventional airframe materials such as an aerospace aluminum, alloy grain size is controlled by special alloying elements (Walsh, Jata et al. 1989) which have a low solid solubility limit at high temperatures and hence precipitate out during casting of the alloy. Titanium for example is normally added to castings to control the grain size in the casting. Also, very small amounts of grain size controlling elements such as Manganese, Chromium, Scandium and Zirconium are added to control grain size and grain shape developed during primary processing of commercial aluminum alloys. Zirconium and Scandium are the most effective elements as they form coherent dispersoids, example: Al_3Zr (dispersoid is a second phase that is dispersed in the matrix). They are also very effective in preventing recrystallization. The radius (r) and the volume fraction (f) (the fraction of space occupied by the second phase) of these high melting point dispersoids are key parameters. In general, the smaller the radius of these particles and the larger their volume fraction, the smaller is the grain size. All modern aerospace Al alloys contain Zirconium, and the aluminum product forms (therefore components) are in an unrecrystallized form. A rolled thick plate aluminum structure has elongated grains in the rolling direction. Grain elongation occurs during hot rolling of the cast ingot into a plate product form. Any deviations from the specified Zirconium content for example would lead to undesirable grain size either in the form of too much recrystallization or large undissolved Zirconium-containing particles.

Apart from the grain size, a second factor that controls plastic deformation is the presence of second phase particles. As mentioned above, most aerospace alloys have several different alloying additions to meet strength requirements and to provide the ability to carry the desired load. The second phase particles that provide the strength are generally termed as strengthening phases or precipitates. Additions of Zinc and Copper in combination with Magnesium result in the formation of precipitates that provide the necessary strengthening in Aluminum alloys. Many high strength alloys, 7xxx and 2xxx series, (designations classified according to major alloying elements, 7– Mg/Zn, 2-Cu) used in military and commercial aircraft contain these elements. Dislocations are line defects, whose propagation results in plastic deformation. In a material with precipitates, the dislocations either cut through these obstacles or by-pass them by leaving loops of dislocations around them. When dislocations shear these precipitates, the strength of a material increases

with the increase in volume fraction and radius of the precipitate. When precipitate sizes exceed a "cut-off radius" they are too large to be cut by dislocations. Below the cut-off radius, the precipitates remain coherent with the matrix. When the precipitates grow and become incoherent with the matrix, the precipitates exceed the "cut-off" radius. This causes dislocations to by-pass the precipitates during deformation resulting in lower strength. The strength in the cutting regime (i.e. the regime where dislocation cuts through the precipitate) is determined by a variety of factors. The most prominent effect arises from the APB (antiphase boundary) energy in the case of ordered precipitates. The coherency strain (mismatch in lattice parameter between matrix and precipitate) plays a significant role in some systems. Other factors include the volume fraction, size of the precipitates, and friction stress in the matrix and precipitate. Equations describing these multiple effects can be quite complex (Parthasarathy, Rao et al. 2004). In the case of the bypass regime, the strength is dependent on fewer factors. This can be given as:

$$\sigma_y = \alpha G b / l \qquad l = 2r/f^{0.5} \qquad \ldots \quad (2)$$

where l is the distance between precipitates, r the radius of the precipitates, f is the volume fraction, a geometrical factor typically equal to 0.5, G is the shear modulus, and b is the Burgers vector of the dislocation, typically half the lattice parameter.

The second phase/precipitate particles lose their ability to contribute to yield strength of the material when they exceed a certain size. In many aluminum alloys, for example, this loss in strength can occur at prolonged exposures at approximately 300 F/150C due to severe coarsening of the precipitates (severe over aging). The coarsening characteristics at temperature depend on the individual alloy and the precipitate-forming elements. Many of the designated tempers (such as T3, T6, T8 and T7) refer to the extent to which the alloys have been aged at temperatures prior to use. Each temper thus corresponds to a prescribed strength, and thus different tempers are suitable for different applications. Any deviation from the temper can be monitored either through electrical conductivity changes or hardness measurements. However, at present, an on-line monitoring of structures through these factors does not exist. It may be possible to develop such instrumentation, and such metallurgical information can be exploited when developing sensors for microstructure sensing applications.

2.2 CREEP DEFORMATION AND RUPTURE

Failures at high temperatures (<0.5 melting point of material in ^{0}K) due to deformation caused by creep are not uncommon. Usually components are not permitted to deform beyond a certain amount of strain or thermal plasticity over a certain period of time under an applied load. For such design problems, creep data in the form of stress versus strain rate (available for many materials) are used. From such a plot (and considering service load conditions), a component can be designed so that thermal plasticity does not exceed the designated value. As discussed above, in some instances the amount of creep deformation is not critical, but failure by creep rupture has to be avoided (such as in the case of a pipe carrying a hot fluid where a certain amount of deformation can be tolerated, but not creep rupture of the pipe). Creep rupture data, i.e. stress vs. time to creep rupture, at desired temperature are typically used. As shown in Table 1, to avoid such failures, stress, time and temperature are key variables, and their effects need to be understood.

The dominance of specific creep deformation mechanism in any alloy is dependent on the applied stress and temperature (Hertzberg 1989). Constitutive equations for each creep mechanism are readily available, and by solving these equations over desired temperature and stress ranges they provide the strain rates which can be plotted as iso-strain rate contours in Ashby map, see Figure 1.

Under high stress and at high temperatures, creep rates are determined by what is termed a 'power law' or 'dislocation creep', regime where the creep rates vary with stress rapidly, as given by:

$$\frac{d\varepsilon}{dt} = A\exp(-\frac{Q}{RT})(\sigma - \sigma_{th})^n \qquad \ldots \quad (3)$$

where ε is the creep strain, t the time, A is a material constant, Q is the activation energy for creep, R is the universal gas constant, σ is the applied stress, σ_{th} is a threshold stress that depends on microstructural state of the material.

At lower stresses, creep rates vary linearly with stress and are said to be undergoing 'diffusion creep'. Within this regime, at higher temperatures, the creep rate is determined by a mechanistic regime termed as the 'Nabarro-Herring' creep regime. The creep rate in this regime is given as:

$$\frac{d\varepsilon}{dt} = 10\frac{\sigma\Omega}{kT}D_{L,o}\exp(-\frac{Q_L}{RT})\frac{1}{d^2} \qquad \ldots \qquad (4)$$

where O is the atomic volume, k the Boltzmann's constant, D_{Lo} the pre-exponent for bulk diffusion of atoms, Q_L the activation energy for bulk diffusion, and d is the grain size. At lower temperatures, the creep is limited by 'Coble' creep and the rate is given as:

$$\frac{d\varepsilon}{dt} = 47\frac{\sigma\Omega}{kT}(\delta_b D_{b,o})\exp(-\frac{Q_b}{RT})\frac{1}{d^3} \qquad \ldots \qquad (5)$$

Where $D_{b,o}$ is the pre-exponent for grain-boundary diffusion, δ_b is the grain boundary width and Q_b is the activation energy for grain boundary diffusion.

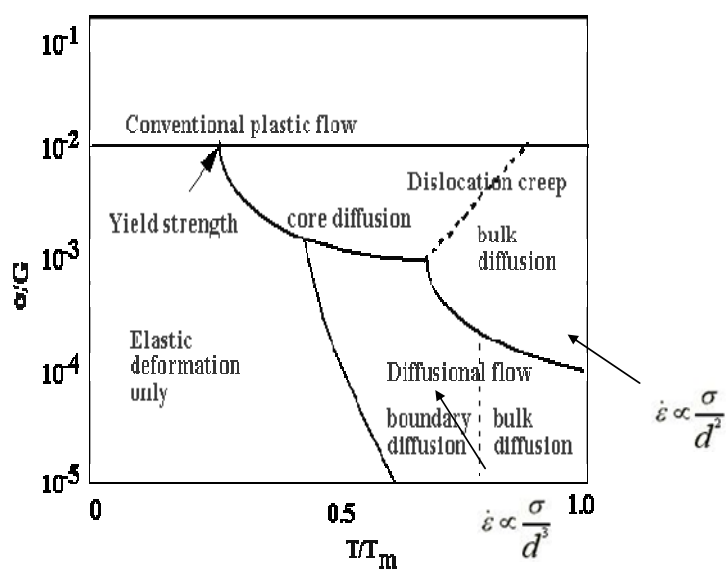

Figure 1. A notional creep deformation mechanism map showing iso-creep strain rate contours, and creep mechanisms that can occur in a metallic alloy under applied stress and temperature.

The iso-strain rate contours in a plot of applied stress (normalized with respect to shear modulus) vs. operating temperature (normalized with respect to melting temperature) (in ^{0}K) represent boundaries that delineate different creep mechanisms. For example as shown in Figure 1, at low stresses and high temperatures Nabarro-Herring creep deformation dominates, where atomic diffusion takes place from boundaries normal to the stress axis to boundaries parallel to the stress axis. Vacancies diffuse in the opposite direction, i.e. from boundaries parallel to the stress axis to boundaries perpendicular to the stress axis. It is important to note here that the microstructural factor that governs the creep strain rate in this regime is proportional to $1/d^2$. At even lower stresses, creep deformation occurs through vacancy migration but along grain boundaries and the strain rate is very sensitive to the number of grain boundaries through a $1/d^3$ relationship. There is no dislocation motion in these high temperature and low stress regimes, and no grain elongation occurs. Grains however rotate resulting in a loss of the original texture and grain boundary sliding occurs. At higher applied stress levels, creep is controlled by dislocation movement and is

independent of grain size, shown as dislocation creep regime in Figure 1. Grains here elongate and new textures form. Currently, in order to decipher the specific mechanism that is occurring in a component, specimens from the component are sectioned and prepared for scanning or transmission electron microscopy observations. Voids, grain size/orientation modification and formation of new textures can then be studied and documented for almost any material component after the failure has occurred. NDE-based sensing for on-line health monitoring can focus on developing sensors to monitor the above mentioned microstructural parameter-changes in real time.

2.3 STATIC FRACTURE

In today's aerospace designs there are very few metallic components that fail purely due to a static overload mechanism. However, overload fracture can occur after a crack has first grown by a different fracture mechanism, for example by fatigue or stress corrosion. In such a case a crack grows to a critical crack size by such a mechanism, and then the final fracture occurs by overload. Rather than using material elongation or %ductility obtained using smooth bars, fracture toughness (K_{1c}) is used as an engineering indicator for a material's ability to withstand overloads under brittle conditions or plane strain loading conditions.

In order to obtain K_{1c} fracture toughness for the material is estimated for the most brittle condition (thick-gage or high strain rates or temperatures below ductile to brittle transition temperature will provide the lowest fracture toughness) encountered during service. For metals, an atomically sharp crack is imbedded in a fracture mechanics specimen and fracture toughness is evaluated using an approach outlined in the ASTM (American Society for Testing of Materials) standard E399. J_{1c} (elastic-plastic fracture mechanics parameter) is used when the material exhibits considerable plasticity during loading and crack extension and linear elastic fracture mechanics is not applicable. Tearing modulus defined as dJ/da, represents crack growth toughness and has been evaluated recently as an additional parameter to evaluate material fracture resistance. For thin sheet materials, such as the material gage used for aircraft fuselage, R-curves (crack resistance behavior) are generated on very large specimens, indicative of large thin structures because small specimens do not provide realistic values. The procedure to obtain an R-curve is also given in the ASTM standards.

Figure 2 summarizes various microstructural parameters that govern fracture toughness and tearing modulus for precipitation-hardened aluminum alloys used routinely for aircraft structures (Jata, Vasudevan, 1998). As shown in this Figure, fracture initiation toughness (K_{1c}, J_{1c}) and crack growth toughness (same as Tearing Modulus, T_r) decrease with increase in yield strength. In this Figure, UA refers to under aged material and PA refers to peak aged material that has higher yield strength than UA. The Figure also attempts to illustrate that, for constant yield strength, as microstructural parameters such as grain size, strengthening precipitates and impurity content are refined (reduced in size or extent), $K_{1c,}$ J_{1c} and T_r increase. Fine second phase particles improve homogeneity of slip, thereby improving fracture toughness parameters. Homogeneity of slip also promotes ductile failure, void nucleation and growth. Larger grain boundary precipitates and impurity particles (also known as inclusions) decrease toughness through promotion of brittle fracture.

Thus grain size, strengthening phases and second-phase particle distribution play a key role in fracture initiation toughness and crack growth toughness of many engineering alloys through control of slip mode or dislocation processes that are ultimately responsible for the amount of plasticity that a material can accumulate prior to fracture. By sensing plasticity parameters during operational service or by sensing the microstructural factors prior to or during service, microstructure-based structural health monitoring would provide key information regarding static fracture conditions, material toughness and remaining strength.

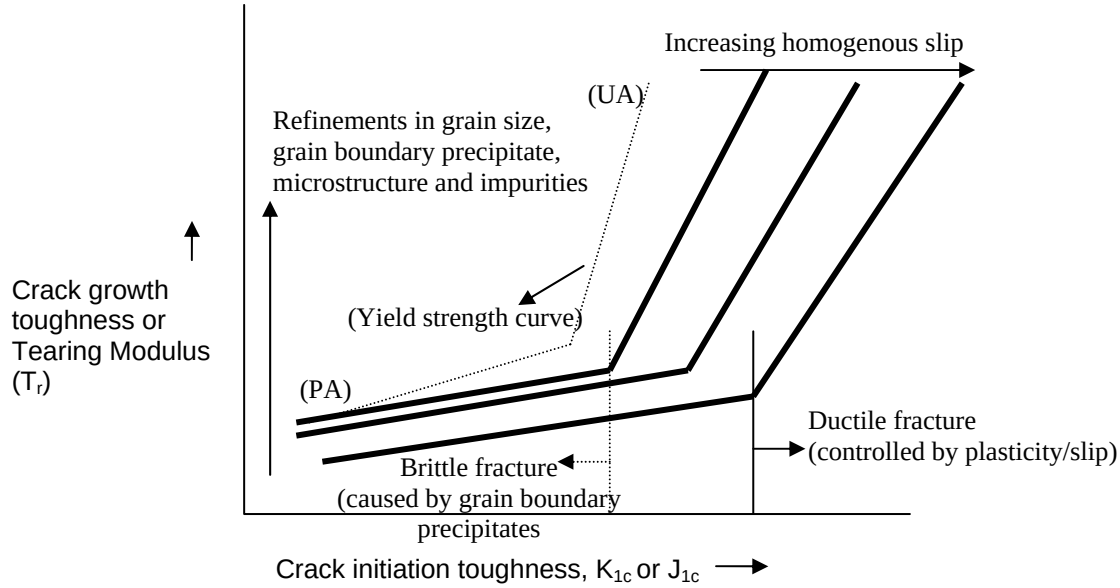

Figure 2. Relationship of crack initiation toughness and tearing modulus (or crack growth toughness) to various microstructural parameters in precipitation-hardened aluminum alloys

2.4 DYNAMIC FATIGUE

Fatigue is one of the dominant modes of failure, and it has been investigated more thoroughly than any other fracture mechanism, where numerous papers have been published in the technical literature. For this paper, the aim is to present a basic summary of the microstructural parameters that control fatigue crack growth. As discussed earlier, applied stress-range and strain-range are the key parameters that dictate how long a laboratory specimen or a component will survive as a function of applied cyclic loads.

When a stress controlled or high cycle fatigue test is performed on a smooth or notched specimen the number of fatigue cycles to failure represents cycles to crack initiation.. The cycles to failure will normally depend on the value R-ratio (the ratio between the minimum to maximum applied load cycle is known as the R ratio (P_{min}/P_{max})). In the case of high-cycle fatigue the maximum applied stress is kept below the yield stress of the material. Cracks almost always initiate on the surface either by fracture of a large inclusion/s or at a grind or a scratch mark due to improper machining of the component. In high-cycle fatigue applications, compressive residual stresses are usually imparted on the surface either through shot peening (blasting the surface with fine particles to impart compressive residual stress) or most recently by laser shock peening to increase the number of cycles to failure, however the compressive residual stresses usually decay with fatigue cycling and are not a permanent solution to the fatigue failure problem. The key microstructural parameter in high-cycle fatigue is the size of the largest inclusion or the range of size of inclusions that will participate in the initiation of fatigue fracture.

In strain-controlled fatigue, a specimen is cycled within a prescribed strain range that could be below or above the yield of the material. Cyclic plasticity is accumulated as the specimen is cycled and the total accumulated cyclic plasticity dictates the (low-cycle) fatigue cycles to failure. Here plasticity is accumulated through slip or dislocation movement from the bulk of the material to the surface. Cracks initiate in slip bands and eventually link up causing failure. The Coffin-Manson law relates the applied plastic strain amplitude, ($\Delta\varepsilon_p/2$) to the number of strain reversals, $2N_f$ to failure as given by:

$$\frac{\Delta\varepsilon_p}{2} = \varepsilon_f^{'}(2N_f)^c \qquad \ldots \qquad (6)$$

where $\varepsilon_f^{'}$ is the fatigue ductility coefficient (it is the value of the plastic strain amplitude when failure occurs in one strain reversal) and c is the fatigue ductility exponent (obtained by the slope of the line that relates the plastic strain amplitude to the reversals to failure.)

However, a more important problem in structural failures is failure through fatigue crack propagation. Here the assumption is that when a component is inserted into service after nondestructive evaluation (NDE) inspection, a crack population below the resolution limit of the NDE equipment will go undetected. Hence cracks below the resolution limit of the NDE equipment being used are assumed to be present in the structure and the fatigue crack growth law for that particular material in question is applied to estimate the number of cycles that will be needed to grow the crack or cracks to a critical crack size and cause failure. For airframe structures it is common to assume that a 30 mil crack (0.762 mm) will go undetected. This number can easily become much bigger if the structure is complex from a point of view of number of material layers and the presence of sealants. (Many of the complex aerospace structures are made up of multi-layers, sometimes up to five, separated by corrosion prevention compounds known as sealants; the multi-layers can also be separated by shims with the structure held together by fasteners which may or may not be of the same material as the multi-layers. All these factors make the detection, location and sizing of the cracks extremely difficult, particularly when the NDE inspection is performed without disassembling the aircraft.) Unlike airframe structures, a small flaw present in a rotating turbine engine component can create a major loss of the entire engine or even loss of the aircraft. Thus study of small cracks (cracks whose dimensions are of the same order as that of the grain size of the material or less) is of extreme importance in materials that are used for gas turbine engine. A number of investigations have been performed to understand small crack growth behavior with respect to microstructure, residual stress and grain size. The reader is referred to the article, "Relevance of small crack problem to lifetime prediction in gas turbine engines,"(Lankford and S J Hudak 1987) as a starting point for this subject. Fatigue crack growth rates (da/dN, where da is the increment in crack size and dN is the increment in number of applied load cycles) for larger cracks for a few contrasting materials are shown in Figure 3 as a function of the stress intensity range $\left(\Delta K = \Delta\sigma\pi\sqrt{a}\right)$ also termed the crack driving force (Ritchie and Gilbert et.al 2000). When the crack growth rate decreases to very small values below 10^{-10} m/cycle the corresponding stress intensity range is designated as ΔK_{th} and known as the fatigue threshold stress intensity range. In Figure 3 the curve designated as "Striation model" refers to the "Paris law" shown below through equation (7). Many aircraft structural components are designed for fatigue crack growth rates corresponding to those in region II of the fatigue crack growth curve where Paris' law is obeyed and the fatigue crack extends by a striation mechanism given by equation (8) below,

$$\frac{da}{dN} = \left(\Delta K\right)^m \qquad \ldots \quad (7)$$

$$\delta = \beta\left(\frac{\Delta K^2}{E\sigma_{YS}}\right) \qquad \ldots \quad (8)$$

where δ is the crack tip opening displacement related to crack growth rate per cycle in the material and β is a constant. In Figure 3, brittle materials such as amorphous glass and alumina exhibit very small crack opening displacement and hence need lower driving force or stress intensity range to extend the fatigue crack growth. In the case of materials such as high strength steels and aluminum alloys the stress intensity range to grow the cracks is larger. Note that the crack opening displacement for a given stress intensity range is related to the fundamental material parameters, elastic modulus (E) and yield strength (σ_{ys}) of the material.

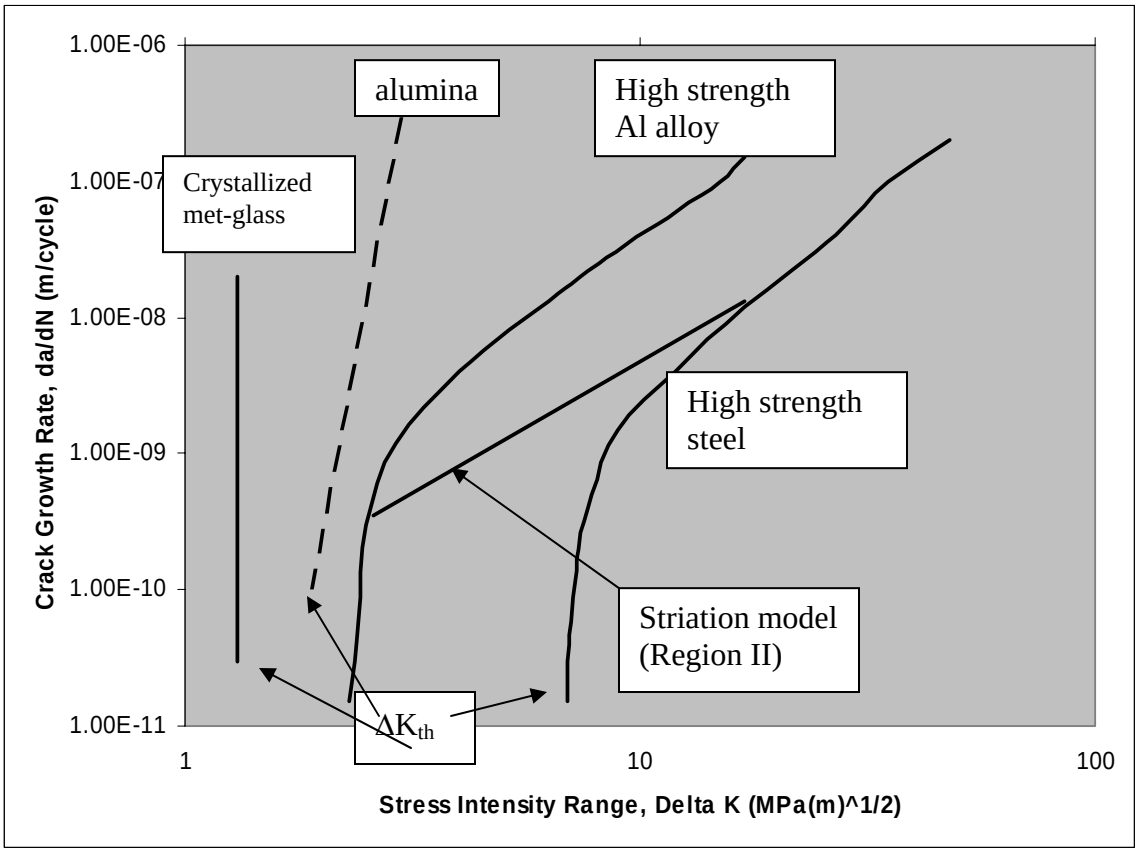

Figure 3. Fatigue crack growth rate vs. stress intensity range of a number of materials. Striation models use the Paris law equation.

As mentioned above, for the lower end of the stress intensity range, crack growth rates asymptotically decrease to very small values corresponding to rates that lie in the range of 10^{-11} m/cycle, and the stress intensity range reaches a fatigue threshold stress intensity ΔK_{th}. In this low end regime, fatigue crack growth rates are strongly influenced by microstructural parameters such as grain size and second phase particles. In engineering materials it is often difficult to separate the effect of grain size from other microstructural parameters such as second phase particles. Nevertheless, in precipitation hardened aluminum alloys it is shown that for a constant grain size fatigue crack growth resistance is superior when strengthening phases are coherent (under-aged alloys) and is inferior when they are incoherent (over aged Al alloys). This has been shown to be directly related to slip characteristics and nonlinearity of the crack path in the material. When particles are coherent crack tip plasticity is accumulated through planar slip and the fatigue cracks follow slip planes resulting in a crack path that has many tilts and when incoherent particles are present non-planar slip dominates, which results in a much straighter crack path. The out of plane crack path (made up of tilted cracks) provides a much higher fatigue crack growth resistance. Similarly fatigue threshold intensity range has also been shown to have a direct relationship to particle spacing and particle volume fraction. Widely spaced particles and lower volume fractions cause increased out of plane of cracking resulting in larger fatigue thresholds (Carter, Lee et al. 1984; Jata and E A Starke 1986; Vasudevan, Sadananda et al. 1997,Ritchie, Gilbert et al. 2000).

Recently, a comparative study of grain size effects on crack propagation in nickel was performed (Hanlon, Tabachnikoya et al. 2005). The study showed that the nickel containing nano sized grains has the least amount of non-linearities in crack path and the fastest crack propagation rates. Fatigue cracks in the microcrystalline and conventional nickel with larger grains propagated with much more out-of-plane tilts providing slower fatigue crack growth rates. Also recently, fatigue threshold intensity for a number of important engineering alloys were compiled and analyzed and it was shown that the threshold stress intensity range increases with grain size (Sadananda and Vasudevan 2003). As shown here the subject of fatigue is vast and the microstructural relationship to fatigue crack growth rate is clearly material dependent. Therefore for prognosis it is essential to know the material and its microstructural state so that the fatigue crack growth law corresponding to that particular material and material state in question is applied. As future materials are required to operate in more extreme environments microstructural changes may take place during a mission where crack growth behavior will alter during a mission. Therefore, the future endeavors in development of sensors for material and damage state awareness must target microstructure parameters that control fatigue crack growth.

2.5 CORROSION

Uniform corrosion (it should be recognized that this term is routinely used in the corrosion literature and does not necessarily imply uniform corrosion; in a given structure there may be a large variation in the extent of so called uniform corrosion) mentioned previously is just one form of corrosion. This form of corrosion does not impact structural integrity initially, but can impact structural integrity if too much loss of material occurs. There are at least seven additional forms of corrosion (Jones 1992) and of these the ones that affect the aerospace structures the most from a structural integrity point of view include pitting corrosion, environmentally assisted cracking (EAC), intergranular corrosion. Stress corrosion cracking, corrosion-fatigue, and hydrogen embrittlement fall under the category of EAC and when they occur can lead to very costly failures.

In the case of stress corrosion cracking, an existing crack in a material propagates under the combined influence of stress and corrosion environment. The fracture toughness of the material is not altered due to the environment but an existing crack can reach the critical crack size (in a general sense $K_{1C} = \sigma\sqrt{\pi a_{cr}}$) through the combined influence of stress and environment. Fracture mechanics test methods exist to evaluate the threshold, K_{1scc} or K_{1EAC} (where EAC refers to environmentally assisted cracking), (and the subscript "1" refers to mode 1 tensile loading) below which stress corrosion cracks will not propagate. The two regimes, "Region 1" and "Region II", of stress corrosion cracking in fracture mechanics specimens or structures containing atomically sharp cracks are shown schematically in Figure 4. Numerous reports exist in the literature for Al and Ti alloys where microstructure has been shown to play a dominant role. High strength aerospace aluminum alloys have been investigated thoroughly for stress corrosion cracking (SCC) in 3.5% NaCl (sodium chloride) solution. This electrolyte is of much interest since chloride ions contained in NaCl solution degrade aluminum alloys significantly. A compilation of stress corrosion crack growth rates for 7079, 7039, 7049, 7075 and 7050 shows that the crack growth velocity (da/dt in m/s) are almost similar in the T-7 temper, approximately $8*10^{-10}$ m/s. T-7 is the over aged temper. However, many of the older aircraft (aging aircraft) use 7049, 7079 and 7075 in T6 temper that corresponds to high strength condition (peak aged) and were not optimized for stress corrosion cracking. In this temper the stress corrosion crack velocity is much faster than $8*10^{-10}$ m/s. In alloy 7079-T6 the SCC cracks grow at 10^{-5} m/s and in 7075-T6 SCC cracks propagate at 10^{-8} m/s. However, results in the literature show that the effect of aging (of aerospace aluminum alloys) on the stress corrosion cracking resistance is not that straight forward. The effect depends on the chemical composition of the alloy. For example in some high strength aerospace aluminum alloys it has been shown that over aging (i.e. microstructure containing incoherent precipitates) can improve stress corrosion cracking thresholds, whereas in some other alloys the thresholds were not

affected but the plateau velocity in region II of the stress corrosion crack growth rate vs. stress intensity was drastically improved using over aging methods (Spiedel 1975).

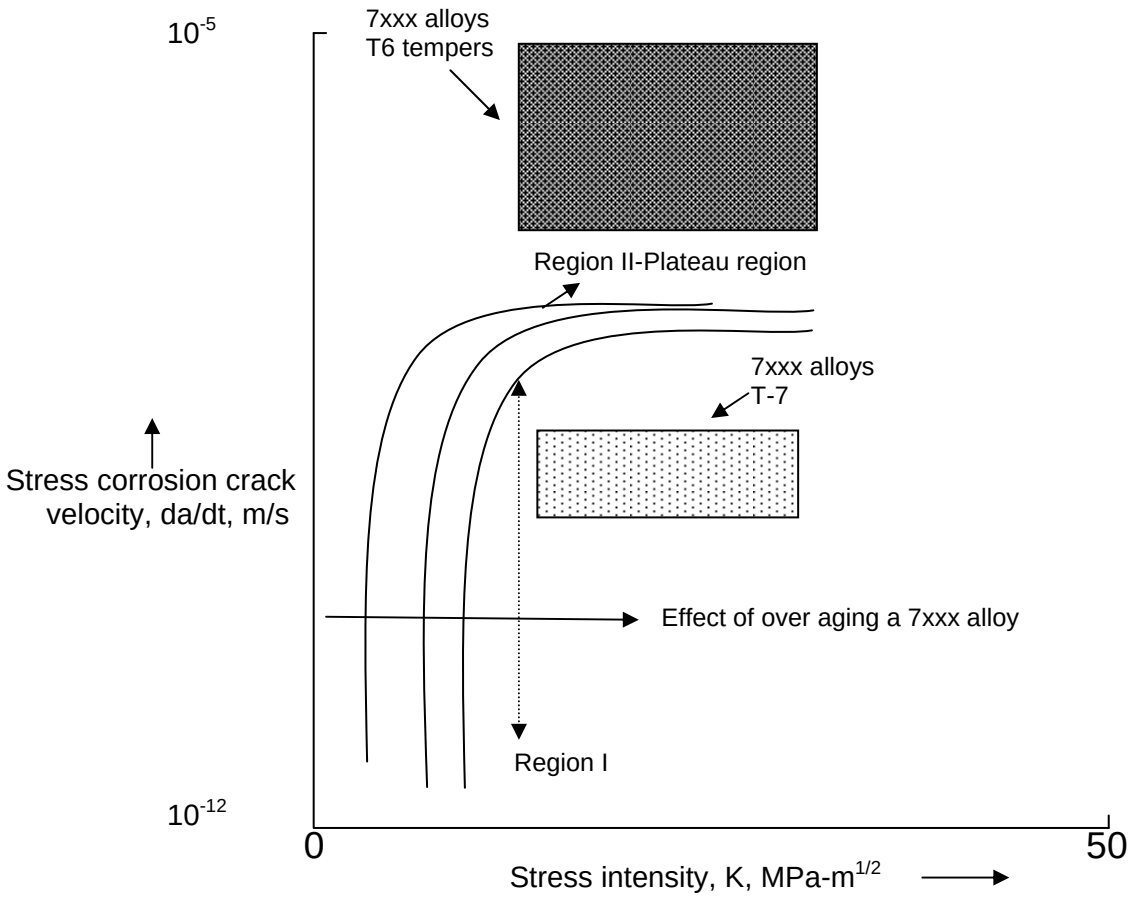

Figure 4. A general representation of stress corrosion crack growth rates as a function of stress intensity in aerospace Al alloys. Also stress corrosion crack growth rates are notionally compared in T6 and T7 tempers.

Also for Aluminum-Lithium (Al-Li) alloys the addition of trace elements has been shown to improve corrosion resistance; for example small additions of Zinc or Indium to Al-Li alloys improve K_{1scc}. The over aged alloys also exhibit improved fatigue endurance limits under high cycle fatigue (stress controlled fatigue) loading conditions. Under corrosion-fatigue conditions in fracture mechanics samples crack growth rates are a function of load cycling frequency. At low frequencies, environmental contributions increase and the crack growth rates vary as a function of frequency. Recently for Ti-8Al-1Mo-1V alloys in 3.5% NaCl solution, it has been shown through analysis of corrosion-fatigue data that environmental contribution to fatigue increases as the frequency decreases (Sadananda and Vasudevan 2005). A parameter that represented environmental contribution was plotted as a function of frequency and it was noticed that this parameter increased linearly as the frequency decreased from 15 to 3 Hz. At 3 Hz the environmental contribution parameter leveled-off. This value was found to be equivalent to the stress corrosion cracking threshold, K_{1scc} of the alloy. Stress corrosion cracks can often be identified as they branch out while branching in general is minimal. Nevertheless careful analysis and experience is required to distinguish the

two. Many of the fracture mechanisms and example fractographs can be found in references (Hertzberg 1989, Jones 1992). Hydrogen can affect crack growth rates in many alloys including Ti-based alloys which are of interest to aerospace industry. In these alloys hydrogen can accelerate crack growth rates by lowering the cleavage fracture stress and or by forming titanium hydrides. The amount of hydrogen required to embrittle the Ti-based alloys depends on the volume fractions of various phases (present in the alloy), stress state conditions at the crack tip, temperature and crack tip strain rate. A large body of information on this subject has been published between 1973 and 1990 and the reader is referred to the text books referenced here in this article.

2.6 OXIDATION

In metallic alloys, material loss at low temperatures is dominated by solid-liquid interactions as discussed under corrosion. At higher temperatures, material loss typically takes place through gas-solid reaction. In most high temperature applications the reactive component in the gas is oxygen. Thus oxidation is primary source of material loss at elevated temperature. The rate at which a metal will oxidize varies drastically from one to another depending upon the chemistry of elements that make up the metallic alloy. In addition the microstructural features also affect the oxidation rates. In a well engineered alloy, the composition is tailored in such a way as to form a very dense, tenacious and adherent film of an oxide on the surface that prevents further oxidation by forming a physical barrier between the gaseous oxygen and the underlying material. For example, aluminum oxide is known to have very low permeability for oxygen. However aluminum itself is low melting and is not a high temperature metal. Nickel has a high melting point and retains strength at higher temperatures, but nickel oxide is not a good barrier to oxygen due to high permeability. Thus an alloy of nickel and aluminum was conceived to take advantage of the high temperature capability of nickel and the oxidation barrier formation property of aluminum.

Real engineering alloys are made of compositions much more complex than just two elements. Thus the oxidation behavior is quite sensitive to the actual composition as well as the microstructure. During service the alloy may change in composition, especially at the surface and in microstructure throughout the material. For example, an engineering alloy of molybdenum and silicon with boron additions makes use of the high temperature capability of molybdenum and the low permeability oxide of silica for the barrier.(Mendiratta, Dimiduk et al. 2002; Parthasarathy, Mendiratta et al. 2002; Parthasarathy, Mendiratta et al. 2002) The silica barrier is formed using the silicon in the alloy, thus depleting the surface of the alloy in silicon. If the surface silica layer is damaged, the silicon content in the substrate may be insufficient to form a barrier once more and protect the bas material. If a method by which the composition of the substrate underneath oxide layer can be measured, then it will be possible to predict the remaining life of the alloy. Properties that are sensitive to chemistry need to be identified and suitable measurement transducers invented for such applications.

In the current generation of nickel-based superalloys, the alloys are protected from a thermal barrier layer of zirconia. This barrier layer is however permeable to oxygen. The oxygen reacts and forms alumina beneath the thermal barrier. As this alumina layer grows in thickness, the thermal barrier becomes unstable and eventually spalls (fractures and falls off).(Sergo and Clarke 1998; Wang and Evans 1998) This is a clear material failure resulting in overheating of the Ni-based alloy underneath. It will be of great engineering use, if a method to measure the thickness of the alumina that forms under the thermal barrier layer is available. The dependence of the alumina layer thickness on the remaining life of the barrier layer is already known; thus it remains to come up with a method to measure in-situ the alumina thickness beneath the thermal barrier layer.

2.7 PHYSICS OF FAILURE OF CERAMIC MATRIX COMPOSITES

Ceramics offer significantly higher temperature capabilities than metals. In general, ceramics have a higher melting point and thus better creep resistance, along with good resistance to environmental attack such as corrosion. Among the ceramics, the oxides are particularly attractive since they are also inherently stable against oxidation at temperature.

Ceramics, however, are inherently brittle, by which it is meant that they suffer very low total mechanical strain (typically 0.1%) before failure. This is due to their inability to absorb mechanical energy when subjected to mechanical forces. It is possible to make ceramics that are very strong, and this is usually accomplished by careful processing that will limit the flaws in the material to a very small size. However it is impossible to ensure that new flaws are not introduced during service, often from what is termed 'foreign object damage.' When such unexpected mechanical loads result in flaws, the ceramic typically fails catastrophically without absorbing significant energy. This insidious failure is the only factor that is keeping us from using these otherwise very attractive materials. Even if flaws that appear during service are 'sensed' using NDE methods, it may be too late to prevent failure.

This debilitating disadvantage of ceramics has been recently alleviated by the concept of fiber-reinforced ceramic composites. In this concept, ceramics are processed in such as way as to make very fine diameter fibers of very high strengths. Typical fibers are 10 microns in diameter and possess failure strengths of 2-3 GPa. Once again, the fibers themselves have flaws of varying sizes and the weakest flaw is limited in size to achieve these strengths. Depending on the modulus, these fibers have failure strains of the order of 0.5 to 1%. These fibers are then encased within a ceramic matrix of normal strength (with failure strains of ~0.1%). The fibers and the ceramic matrix may be separated by an interfacial layer to prevent the cracks in the matrix from entering the fibers and causing premature failure. In some cases the matrix is so weak that no interfacial layer is required (Kerans, Hay et al. 2002; Parthasarathy and Kerans 2003). The key engineering aspect in the design of these materials is to protect the fibers from premature failure by the cracks in the matrix. Once the fibers are thus protected, they bridge the cracks in the matrix and offer resistance to their propagation (figure.5a) The fibers themselves fail eventually at some higher load, and since their failure location is different from that of the matrix, they are pulled out of the matrix, as in a piece of wood. This amounts to significant absorption of energy, which imparts high reliability and resistance to 'foreign object damage' to the composites.

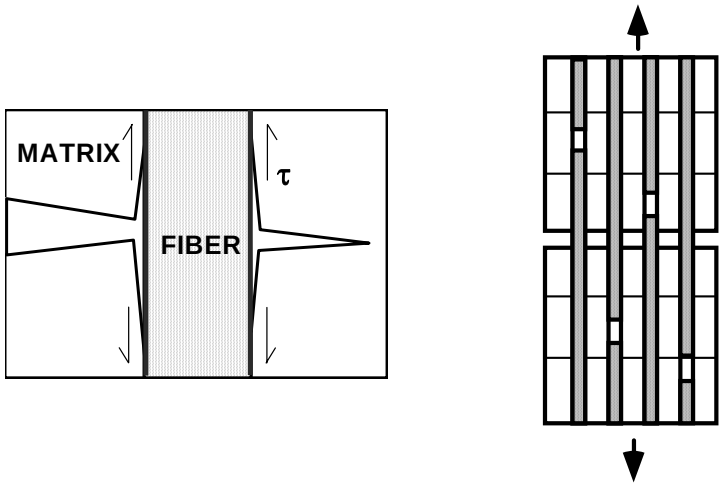

Figure 5 (a) the fibers in ceramic composites bridge the cracks in the matrix and offer resistance to their propagation (b) the fibers eventually fail and pull out of the matrix absorbing significant energy imparting high reliability as in wood.

The application of ceramic composites in real high temperature structural applications has just begun. It is anticipated that they will be used widely as the designers gain confidence in using them. As this class of

materials begins to find applications, the NDE methods will need to come up with techniques to predict their remaining life during service from parameters that can be measured in-situ.

Referring back to Table I, which summarizes the usual failure mechanisms of materials, with respect to ceramics, ceramic composite failures are almost invariably dominated by fracture. In certain applications, material loss is also a concern. The following will focus on fracture mechanisms and highlight a few of the dominant mechanisms of material loss.

2.7.1 Fracture

Mechanical loads and fatigue :

The fracture of a unidirectional ceramic composite in uniaxial tension was explained briefly in the previous section. In real applications, ceramic composites are built with various fiber architectures and the stress states are far more complex, both of which result in various different forms of failure. A typical CMC is now made from fabrics that are woven using tows (bundles of fiber filaments). The fabric has fibers running along two perpendicular directions as in most cloths. In a typical CMC, these cloths are stacked and the gaps filled with a matrix. The complex fabrication methods and the high refractoriness of ceramics in general result often in incomplete densification of the matrix. This complex fiber architecture and the difficulty of densifying ceramics results in a matrix of varying porosity throughout the composite. When subjected to mechanical loads, the failure starts near these pores and progress across the composite in a distributed way. This often results in externally measurable modulus changes. It is quite possible that NDE methods could be devised to measure this modulus changes in-situ thus providing the first possibility of estimating damage progression during service in these materials.(Zawada, Butkus et al. 1991; Zawada, Hay et al. 2003).

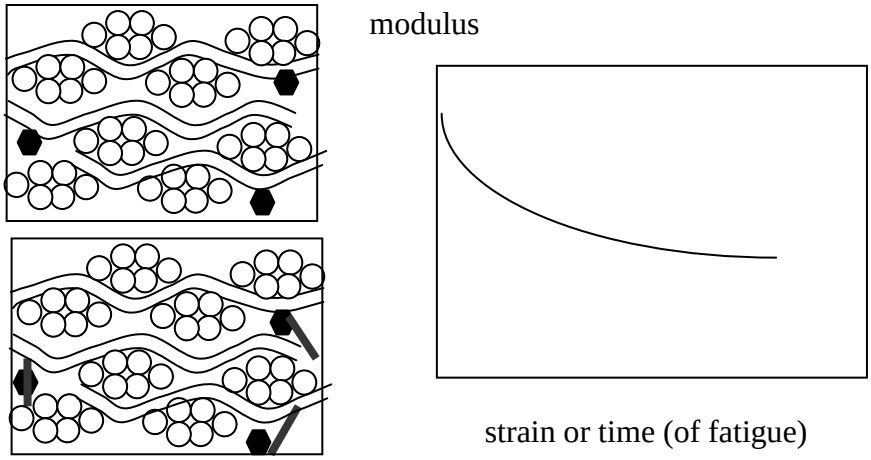

Figure 6: (a) the complex architecture of CMCs and the inhomogeneous porosity/defect distribution in the matrix leads to distributed damage (cracks) in the material, which reflects as (b) loss of macroscopic modulus of the material with strain (during a tension test) or with time (during a fatigue test).

The damage that occurs in a CMC during use can also be measured using hysteresis loss(Morscher and Gyekenesi 1998). The fibers that slide against the matrix holes result in frictional wear at the interface. With time the frictional resistance decreases. This is often reflected in the loss of hysteresis during a cyclic stress-strain test. With NDE methods it may be possible to sense internal energy-absorbing events and from the variations of these energy absorption mechanisms one may be able to predict the status of damage in the composites and thus the remaining life.

Thermal gradients:

Ceramic composites are often used where very high temperature reactions have to be contained. In addition, ceramics have low thermal conductivity offering protection against undesirable heat loss, which often lowers efficiency. This results automatically in larger thermal gradients across the ceramic composites. The mechanical stresses are typically in-plane while thermal gradients are typically perpendicular to this plane. The thermal gradients cause uneven thermal expansion of the material through the thickness and result in a large driving force for shear cracks to propagate between the 'cloths' of the composites (see Fig.6).

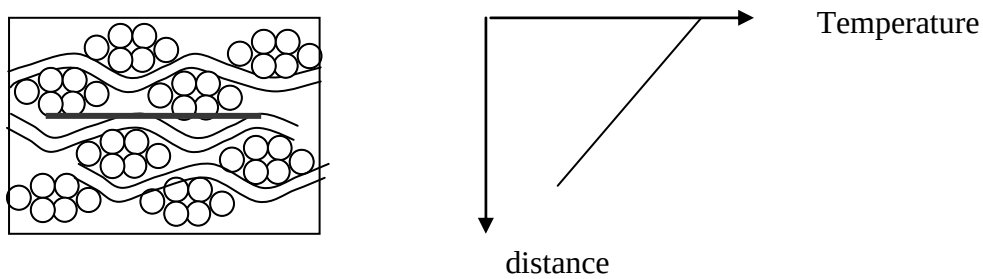

Figure 7: Delamination cracks result from larger thermal gradients often present in service of high temperature structural CMCs.

Delamination cracks are a constant issue in determining the life of CMCs.(Cutler, Zok et al. 1997; Sorensen, Sarraute et al. 1998) A method to detect the delamination cracks early will help significantly in avoiding expensive damages and in predicting remaining useful life of CMCs.

Microstructural Degradation:

Another failure mechanism in ceramic composites is premature fracture arising from degradation of microstructure. The fibers are typically made of fine-grained material in order to keep the processing flaw sizes small. -However fine grains are inherently stable and with time at temperature, the grains grow. As the grains grow, which typically occurs during service, the strength of ceramics decreases(Hay, Boakye et al. 1999). Thus the strength of the as-fabricated composite is not guaranteed after long periods of use at temperature.(Keller, Mah et al. 2003). The measurement of grain growth in ceramic fibers is at present limited to tedious specimen preparation and analysis in a TEM (Transmission Electron Microscopy). While very samples are sufficient to diagnose the problems, the method is definitely not in-situ. Any NDE method that might enable a quick assessment of grain size of ceramic materials might be very useful as life predicting sensor in both monolithic and composite ceramics.

2.7.2 Material Loss:

State-of-the-art ceramic composites are based on carbon or SiC, with oxide-based CMCs beginning to find applications. While oxides are inherently stable against oxidation, both C and SiC can suffer material loss from oxidation. C-based composites are typically 'inhibited' from oxidation through the addition of oxidizing compounds that form a surface barrier layer that keeps oxygen away from the carbon underneath. (Jacobson, Leonhardt et al. 1999) However the barrier layer is by design a viscous fluid and under heavy fluid flow conditions can be leached away leaving the carbon unprotected. The SiC based materials form a silica layer through oxidation that protects further loss of SiC. However, silica is now known to suffer from material loss in the presence of moisture at high temperatures(Opilla, Smialek et al. 1999). Thus under combustion conditions of an aircraft engine, silica loss begins to be an issue above 1200C. Once again, barrier layers are being devised to protect against such material loss. Thus one of the factors that determine life of these CMCs is the life of the barrier layer itself. Methods to examine the barrier layer thickness periodically using NDE methods might help prevent unexpected failures and timely replacement of parts.

3.0 SUMMARY

The subject of physics of failure is quite vast and this paper provides a glimpse of the subject. Physics of failure for metals and ceramic matrix composites has been discussed at the material-microstructural level. Readers can further enhance their understanding by going to the references cited below. It is hoped that this paper will provide a direction for developing next generation NDE-based sensors to detect damage in-situ based on fundamental material science principles. An attempt has also been made to bring out the most important features of failure that may help develop better prognosis methods for life prediction of components using important microstructural constituents.

4.0 REFERENCES

Carter, R. D., E. W. Lee, et al. (1984). "The Effect of Microstructure and Environment on Fatigue Crack Closure of 7475 Aluminum Alloy." Met. Trans. **15A**(3): 555-563.

Cutler, W. A., F. W. Zok, et al. (1997). "Delamination Resistance of Two Hybrid Ceramic-Composite Laminates." J. Am. Ceram. Soc. **80**(12): 3029-3037.

Hanlon, E., D. Tabachnikoya, et al. (2005). Int. J. Solid of Fatigue **27**(10-12): 1147-58.

Hay, R. S., E. E. Boakye, et al. (1999). "Grain Growth and Tensile Strength of 3M Nextel 720 after Thermal Exposure." Ceram. Eng. Sci. Proc. **20**(3): 153-163.

Hertzberg, R. W. (1989). Deformation and fracture mechanics of engineering materials, John Wiley and Sons.

Jacobson, N. S., T. A. Leonhardt, et al. (1999). "Oxidative atttack of carbon/carbon substrates through coating pinholes." Carbon: 411-19.

Jata, K. V. and E A Starke (1986). "Fatigue and Fracture Behavior in an Al-Li-Cu Alloy." Metal. Trans. **17A**(6): 1011-1026.

Jata, K. V. and A. K. Vasudevan (1998). Mater. Sci. Eng. **A241**: 104-113.

Jones, D. A. (1992). Principles and prevention of corrosion, Prentice Hall.

Keller, K. A., T. Mah, et al. (2003). "Effectiveness of Monazite Coatings in Oxide/Oxide Composites in Extending Life after Long-Term Exposure at High-Temperature." J. Am. Ceram. Soc. **86**(2): 325-332.

Kerans, R. J., R. S. Hay, et al. (2002). "Interface Design for Oxidation Resistant Ceramic Composites." Jl of the Amer. Ceram. Soc. **85**(11): 2599-2632.

Lankford, J. and S J Hudak (1987). "Relevance of the small crack problem to lifetime prediction in gas turbines." **9**(2): 87-93.

Mendiratta, M. G., D. M. Dimiduk, et al. (2002). "Oxidation Behavior of Mo-Mo3Si-Mo5SiB2 (T2) Three Phase System." Intermetallics **10**: 225-232.
Morscher, G. N. and J. Z. Gyekenesi (1998). "Room Temperature Tensile Behavior and Damage Accumulation of Hi-Nicalon Reinforced SiC Matrix Composites." Ceram. Eng. Sci. Proc. **19**(3): 241-249.
Opilla, E. J., J. L. Smialek, et al. (1999). "SiC Recession Caused by SiO2 Scale Volatility unde Combustion Conditions: II, Thermodynamics and Gaseous Diffusion Model." J. Am. Ceram. Soc. **82**(7): 1826-1834.
Parthasarathy, T. A. and R. J. Kerans (2003). Failure of Ceramic Composites. Fundamental Theories and Mechanisms. I. Milne, R. O. Ritchie and B. Karihaloo, Elsevier Science. **2**.
Parthasarathy, T. A., M. G. Mendiratta, et al. (2002). "Oxidation Mechanisms in Mo-Reinforced Mo5SiB2(T2)-Mo3Si Alloys." Acta Mater. **50**: 1857-1868.
Parthasarathy, T. A., M. G. Mendiratta, et al. (2002). Oxidation Protective Coating for Mo-Si-B Alloys. US Patent #6,340,398. USA, Air Force Research Laboratory.
Parthasarathy, T. A., S. I. Rao, et al. (2004). "A Fast Spreadsheet Model for the Yield Strength of Superalloys." Superalloys 2004, Ed. K. A. Green et al.: 887-896.
Ritchie, R. O., C. J. Gilbert, et al. (2000). Int Jour. of Solid & Struct. **37**(1-2): 3110-3290.
Sadananda, K. and A. K. Vasudevan (2003). "Fatigue crack growth mechanisms in steels." Int. J. Fatigue **25**(9-11): 899-914.
Sadananda, K. and A. K. Vasudevan (2005). "Fatigue Crack Growth Behavior of Titanium Alloys." Int. J. Fatigue **27**(10-12): 1255-1266.
Sergo, V. and D. R. Clarke (1998). "Observation of Subcritical Spall Propagation of a Thermal Barrier Coating." J. Am. Ceram. Soc. **81**(12): 3237-3242.
Sorensen, B. F., S. Sarraute, et al. (1998). "Thermally Induced Delamination of Multilayers." Acta mater. **46**(8): 2603-2615.
Spiedel, M. O. (1975). Met. Trans. **6A**: 631.
Vasudevan, A. K., K. Sadananda, et al. (1997). "Role of Microstructures on the Growth of Long Cracks." Int. J. Fatigue **19**(1): S151-159.
Walsh, J. A., K. V. Jata, et al. (1989). Acta Met. **37**(11): 2861-71.
Wang, J.-S. and A. G. Evans (1998). "Measurement and Analysis of Buckling and Buckle Propagation in Compressed Oxide Layers on Superalloy Substrates." Acta mater. **46**(14): 4993-5005.
Zawada, L. P., L. M. Butkus, et al. (1991). "Tensile and Fatigue Behavior of Silicon Carbide Fiber-Reinforced Aluminosilicate Glass." J. Am. Cer. Soc. **74**(11): 2851-2858.
Zawada, L. P., R. S. Hay, et al. (2003). "Characterization and High Temperature Mechanical Properties of an Oxide/Oxide Ceramic Fiber/Matrix Composite." J. Am. Cer. Soc. **86**(6): 981-990.